



# Estimated Isotopic Compositions of Yb in Enriched $^{176}\text{Yb}$ for Producing $^{177}\text{Lu}$ with High Radionuclide Purity by $^{176}\text{Yb}(d,x)^{177}\text{Lu}$

Yasuki Nagai<sup>1,2</sup>, Masako Kawabata<sup>1,2</sup>, Shintaro Hashimoto<sup>3</sup>, Kazuaki Tsukada<sup>2,4</sup>, Kazuyuki Hashimoto<sup>2</sup>, Shoji Motoishi<sup>1,2</sup>, Hideya Saeki<sup>2,5</sup>, Arata Motomura<sup>1,2</sup>, Futoshi Minato<sup>3</sup>, and Masatoshi Itoh<sup>6</sup>

<sup>1</sup>Oarai Research Center, Chiyoda Technol Corporation, Oarai, Ibaraki 311-1313, Japan

<sup>2</sup>Quantum Beam Science Research Directorate, National Institutes for Quantum Science and Technology, Tokai, Ibaraki 319-1106, Japan

<sup>3</sup>Nuclear Science and Engineering Center, Japan Atomic Energy Agency, Tokai, Ibaraki 319-1195, Japan

<sup>4</sup>Advanced Science Research Center, Japan Atomic Energy Agency, Tokai, Ibaraki 319-1195, Japan

<sup>5</sup>Radiation Sources Production Section, Chiyoda Technol Corporation, Tokai, Ibaraki 319-1195, Japan

<sup>6</sup>Cyclotron and Radioisotope Center, Tohoku University, Sendai 980-8578, Japan

(Received November 27, 2021; revised January 24, 2022; accepted February 9, 2022; published online March 14, 2022)

Recently, great interest has arisen concerning  $^{177}\text{Lu}$  as one of the most important therapeutic radionuclides for treating neuroendocrine tumors. This has driven demand for  $^{177}\text{Lu}$  with high radionuclide purity produced in accelerators, by using highly enriched  $^{176}\text{Yb}$  samples to develop a variety of  $^{177}\text{Lu}$ -labelled radiopharmaceuticals. In this paper, a method is presented to estimate isotopic compositions of enriched  $^{176}\text{Yb}$  samples required for achieving large-scale production of  $^{177}\text{Lu}$  having high radionuclide purity by the  $^{176}\text{Yb}(d,x)^{177}\text{Lu}$  reaction. These isotopic compositions were estimated using the latest measured excitation functions of the  $^{176}\text{Yb}(d,x)^{177}\text{Lu}$  reaction that were confirmed in this study by measuring the integral yields of the reaction, and a particle transport simulation code. The estimated radionuclide purity of  $^{177}\text{Lu}$  for commercially available enriched  $^{176}\text{Yb}$  sample is over 99% at a deuteron energy of 20 MeV. The method plays an important role in determining isotopic compositions of enriched samples for producing high purity medical radionuclides in accelerators.

## 1. Introduction

Early non-invasive diagnosis and targeted radionuclide therapy (TRT) have been playing an important role in treating patients with a variety of cancers using radionuclide therapy radiopharmaceuticals labelled with various kinds of medical radionuclides.<sup>1)</sup> Radionuclides that emit low-energy  $\gamma$ -rays and/or annihilation  $\gamma$ -rays are used for diagnosis, and that emit charged particles (Auger electron,  $\beta^-$ -ray, alpha particle) are employed for TRT.<sup>2,3)</sup> In treating cancers, a low-dose imaging procedure is performed to obtain necessary pre-therapy information on biodistribution and dosimetry in patients, followed by making higher dose targeted molecular therapy in the same patients. This approach of merging therapeutic and diagnosis (imaging) treatments is now called the theranostics approach,<sup>4)</sup> the concept of which is very important to make a personalized medicine treatment for a specific patient. In fact,  $^{90}\text{Y}$ , a pure  $\beta^-$ -ray emitter with an average  $\beta^-$ -ray energy ( $E_{\text{av}}$ ) of 934 keV, is used with the  $\gamma$ -ray emitting  $^{111}\text{In}$  to treat large solid tumors,<sup>5)</sup> and a variety of low-to-medium energy  $\beta^-$ -ray emitting radionuclides are being developed aimed at treating small tumors.

Recently, considerable interest has arisen in  $^{177}\text{Lu}$  with a half-life ( $T_{1/2}$ ) of 6.65 d owing to successful treatments for patients with a certain type of neuroendocrine tumors using  $^{177}\text{Lu}$ -labelled radiopharmaceuticals.<sup>6)</sup>  $^{177}\text{Lu}$  emits  $\beta^-$ -rays ( $E_{\text{av}} = 134$  keV) and low-energy 113 ( $I_{\gamma} = 6.6\%$ ) and 208 ( $I_{\gamma} = 11\%$ ) keV  $\gamma$ -rays.<sup>7)</sup> Percentages in brackets indicate the absolute  $\gamma$ -ray emission probability ( $I_{\gamma}$ ). Recent studies with the use of two (tandem) therapeutic radionuclides, such as  $^{90}\text{Y}/^{177}\text{Lu}$ -radiopharmaceuticals in combination, provide an overall survival longer than that with a single radioisotope,  $^{90}\text{Y}$ -radiopharmaceutical.<sup>8)</sup> A tandem pair of  $^{67}\text{Cu}/^{177}\text{Lu}$ -radiopharmaceuticals used for treating mice with tumors also demonstrates a significant survival improvement compared

with delivery as a single fraction of  $^{67}\text{Cu}$ - or  $^{177}\text{Lu}$ -radiopharmaceuticals.<sup>9)</sup> These results provide important aspects of  $^{177}\text{Lu}$  utilized for treating a wide variety of cancers.

$^{177}\text{Lu}$  is currently produced in reactors either by the  $^{176}\text{Lu}(n,\gamma)^{177}\text{Lu}$  reaction or by the  $^{176}\text{Yb}(n,\gamma)^{177}\text{Yb} \rightarrow ^{177}\text{Lu}$  reaction.<sup>10,11)</sup> In order to encourage widespread use of  $^{177}\text{Lu}$  for therapeutic applications, the production route of  $^{177}\text{Lu}$  in accelerators has also been studied using proton,<sup>12)</sup> deuteron,<sup>13-16)</sup>  $\alpha$ -particle<sup>17)</sup> and electron<sup>18)</sup> beams. The results of these studies demonstrate that the  $^{176}\text{Yb}(d,x)^{177}\text{Lu}$  reaction has the largest cross section at a deuteron energy ( $E$ ) of about 12 MeV. Hence, hereafter we consider the productions of  $^{177}\text{Lu}$  using deuteron beams because this study aims at a large-scale production of  $^{177}\text{Lu}$  with high specific activity. The specific activity of a radionuclide is one of parameters used to describe a radiopharmaceutical that is defined as an activity per quantity of atoms of a particular radioisotope (usually given in units of Bq/g). It is an important criterion for the efficacy of targeted therapeutic radiopharmaceuticals, especially for receptor or antigen targeting agents; this is because the mass levels of peptides or antibodies that can be used to develop labelled radiopharmaceuticals for therapy are limited due to finite receptor or antigen binding sites. Therefore, for medical use one has to produce radionuclides with high specific activity. Here, it is noted that the specific activity of  $^{177}\text{Lu}$  that is produced by charge-exchange reactions on  $^{176}\text{Yb}$  samples, such as the  $^{176}\text{Yb}(d,x)^{177}\text{Lu}$  reaction and also the  $^{176}\text{Yb}(n,\gamma)^{177}\text{Yb}(\beta^-)^{177}\text{Lu}$  reaction, is expected to be high. This is because carrier-free  $^{177}\text{Lu}$  (i.e., all atoms in a sample contain only one specific isotope of the element) can be obtained from deuteron or neutron-irradiated Yb samples by employing chemical separation methods.<sup>11)</sup> In fact, a specific activity of carrier-free  $^{177}\text{Lu}$  with 4070 GBq/mg is expected to be produced by the  $^{176}\text{Yb}(n,\gamma)^{177}\text{Lu}$



$\text{Yb}(\beta^-)^{177}\text{Lu}$  reaction.<sup>3)</sup> Here, it should be mentioned two things. Firstly, impurity radionuclides of Lu present in  $^{177}\text{Lu}$  that affect the specific activity of  $^{177}\text{Lu}$  cannot be chemically separated from  $^{177}\text{Lu}$ , which requires us to use enriched  $^{176}\text{Yb}$  samples for producing  $^{177}\text{Lu}$  having high radionuclide purity. Secondly, enriched  $^{176}\text{Yb}$  samples generally contain a small amount of Yb isotopes other than  $^{176}\text{Yb}$ , such as the second and third heaviest Yb isotopes,  $^{174}\text{Yb}$  and  $^{173}\text{Yb}$ . In such cases long-lived radionuclides of  $^{174\text{m}}\text{Lu}$  ( $T_{1/2} = 142$  d) and  $^{174\text{g}}\text{Lu}$  ( $T_{1/2} = 3.31$  y) would be produced not only by the  $^{176}\text{Yb}(d,4n)$  reaction, but also via the  $^{174}\text{Yb}(d,2n)$  and  $^{173}\text{Yb}(d,n)$  reactions,<sup>13–16</sup> as discussed later. Hence, in order to produce  $^{177}\text{Lu}$  with high radionuclide purity, appropriate isotopic compositions of Yb in enriched  $^{176}\text{Yb}$  samples should be determined prior to its production. However, experimental studies to produce  $^{177}\text{Lu}$  by irradiating enriched  $^{176}\text{Yb}$  samples with deuteron beams have not yet been conducted. Hence, how the radionuclide purity of  $^{177}\text{Lu}$  depends on the isotopic compositions of Yb present in enriched  $^{176}\text{Yb}$  samples remains an open problem. In this study, a method is presented to estimate the radionuclide purity of  $^{177}\text{Lu}$  for several isotopic compositions of Yb in enriched  $^{176}\text{Yb}$  samples using previously measured excitation functions of the  $^{\text{nat}}\text{Yb}(d,x)\text{Lu}$  reaction; this is discussed below by taking the aforementioned case of  $^{174\text{g}}\text{Lu}$  and  $^{174\text{m}}\text{Lu}$ . For the large-scale production of  $^{177}\text{Lu}$ , sufficiently thick enriched  $^{176}\text{Yb}$  samples will be used. Here, if the excitation function of individual reactions of the  $^{173}\text{Yb}(d,n)$ ,  $^{174}\text{Yb}(d,2n)$ , and  $^{176}\text{Yb}(d,4n)$  reactions and the isotopic compositions of  $^{173}\text{Yb}$  and  $^{174}\text{Yb}$  present in enriched  $^{176}\text{Yb}$  samples are precisely known, the yields of (impurity)  $^{174\text{g}}\text{Lu}$  and  $^{174\text{m}}\text{Lu}$  can be accurately calculated. Namely, when a variety of Lu radionuclides are produced by the  $^{176}\text{Yb}(d,x)\text{Lu}$  reaction, if the excitation functions of individual reactions that produce the Lu radionuclides are precisely known, the isotopic compositions of Yb in enriched  $^{176}\text{Yb}$  samples required to produce  $^{177}\text{Lu}$  with high radionuclide purity can be estimated. In this study, the excitation functions will be derived by referring to previously measured excitation functions of the  $^{\text{nat}}\text{Yb}(d,x)\text{Lu}$  reaction in the deuteron energy range of 2 to 40 MeV.<sup>13–16</sup> However, a problem remains in the previous data; the latest results of the excitation functions of  $^{172}\text{Lu}$ ,  $^{173}\text{Lu}$ ,  $^{174\text{g}+\text{m}}\text{Lu}$ ,  $^{176\text{m}}\text{Lu}$ , and  $^{177}\text{Lu}$  by Khandaker et al. differ from the older ones in some deuteron energy range.<sup>16</sup> Hence, we first measured integral yields of Lu radionuclides by the  $^{\text{nat}}\text{Yb}(d,x)\text{Lu}$  reaction to test the validity of the latest results; the test can be performed by comparing the measured integral yields with integral yields that are estimated using the latest results. Note that theoretical studies of the excitation functions of the deuteron-induced reactions on  $^{\text{nat}}\text{Yb}$  were also performed with nuclear model codes, such as ALICE-IPPE, EMPIRE-II, and TALYS TALYS-1.4. Theoretical results are roughly in agreement with the measured excitation functions at  $E = 2\text{--}40$  MeV, but the absolute values of the cross sections differ from each other.<sup>16</sup> To the best of our knowledge, such a study for estimating the relation between the radionuclide purity of  $^{177}\text{Lu}$  and the isotopic compositions of Yb present in enriched  $^{176}\text{Yb}$  samples has not yet been conducted.

The paper comprises five sections. We report on the measurement of integral yields of Lu radionuclides by the

$^{\text{nat}}\text{Yb}(d,x)\text{Lu}$  reaction in Sect. 2. In Sect. 3 we describe a method to determine the aforementioned individual excitation functions, and compare the integral yields estimated using both the measured excitation functions and individual excitation functions with the measured integral yields of Lu radionuclides. We report on the estimated results of the radionuclide purity of  $^{177}\text{Lu}$  produced by the  $^{176}\text{Yb}(d,x)^{177}\text{Lu}$  reaction with various kinds of isotopic composition of Yb isotopes present in enriched  $^{176}\text{Yb}$  samples in Sect. 4, and summarize this study in Sect. 5.

## 2. Measurements

We measured the integral yields of Lu radionuclides produced by the  $^{\text{nat}}\text{Yb}(d,x)\text{Lu}$  reaction to compare them with those estimated by using the latest measured excitation functions of the reaction.<sup>16</sup> The Lu radionuclides were generated by irradiating a metallic  $^{\text{nat}}\text{Yb}$  sample for 10 min with a  $0.338\ \mu\text{A}$ , 25 MeV deuteron beams that was provided from the azimuthally variable field (AVF) cyclotron at Cyclotron and Radioisotope Center (CYRIC), Tohoku University, in Japan.<sup>19</sup> We used 25 MeV deuteron beams in order to obtain a large integral yield of  $^{177}\text{Lu}$  by referring to the latest result of the excitation function of the  $^{176}\text{Yb}(d,x)^{177}\text{Lu}$  reaction, measured by using  $^{\text{nat}}\text{Yb}$  samples.<sup>16</sup> The  $^{\text{nat}}\text{Yb}$  sample of 1.831 g mass with a thickness of 6 mm that was enough to stop 25 MeV deuterons in the sample was used. A tantalum slit with a diameter of 10 mm was placed before the  $^{\text{nat}}\text{Yb}$  sample. Note that the isotopic composition of  $^{\text{nat}}\text{Yb}$  is 0.1% for  $^{168}\text{Yb}$ , 3.0% for  $^{170}\text{Yb}$ , 14.1% for  $^{171}\text{Yb}$ , 21.7% for  $^{172}\text{Yb}$ , 16.1% for  $^{173}\text{Yb}$ , 32.0% for  $^{174}\text{Yb}$ , and 13.0% for  $^{176}\text{Yb}$ .<sup>20</sup>

Shortly after the end of irradiation (EOI) and 37 days after the EOI, we took  $\gamma$ -ray spectra of the irradiated  $^{\text{nat}}\text{Yb}$  sample with high-purity Ge (HPGe) detectors to obtain the yields of short-lived and long-lived Lu radionuclides, respectively. Isotope assignments of observed  $\gamma$ -rays were made on the basis of their energies and decay curves. In the former measurement the yield of Lu radionuclides with a short half-life, such as  $^{176\text{m}}\text{Lu}$  ( $T_{1/2} = 3.66$  h),  $^{170}\text{Lu}$  ( $T_{1/2} = 2.0$  d), and  $^{169}\text{Lu}$  ( $T_{1/2} = 34.1$  h), were obtained by measuring  $\gamma$ -rays that were emitted from the irradiated ingot  $^{\text{nat}}\text{Yb}$  sample. Here, the self-absorption correction for the  $\gamma$ -rays following the decays of  $^{176\text{m}}\text{Lu}$  ( $T_{1/2} = 3.66$  h),  $^{170}\text{Lu}$  ( $T_{1/2} = 2.0$  d), and  $^{169}\text{Lu}$  in the ingot  $^{\text{nat}}\text{Yb}$  sample was made, as follows. We first determined an average depth,  $d$ , which is given as the distance of the position of the average radioactivity of the irradiated  $^{\text{nat}}\text{Yb}$  sample from the sample surface, and then calculated the attenuation of a  $\gamma$ -ray with an energy of  $E_\gamma$  emitted from the sample by using a photon cross-sectional database provided by the National Institute of Standards and Technology.<sup>21</sup> Here, because the  $\gamma$ -ray self-absorption factor strongly depends on the  $\gamma$ -ray energy, we used a number of  $\gamma$ -rays of well-known relative intensity such as 78.7, 181.5, 203.4, 377.5, 528.3, 810.1, 900.7, and 1093.6 keV  $\gamma$ -rays from the decay of  $^{172}\text{Lu}$  ( $T_{1/2} = 6.70$  d).<sup>16</sup> We accurately determined  $d$  to be 0.34 mm by comparing the  $\gamma$ -ray intensities corrected for the detection efficiency and  $\gamma$ -ray self-absorption with the intensities given in Ref. 16. The calculated yields of  $^{172}\text{Lu}$  using observed  $\gamma$ -ray yields, absolute  $\gamma$ -ray emission probability of  $\gamma$ -rays from the decay of  $^{172}\text{Lu}$  ( $I_\gamma$ ),  $\gamma$ -ray detection efficiency of a HPGe detector



**Table III.** Reaction channels for producing a Lu radionuclide with a mass number B,  ${}^B\text{Lu}$ , by the  ${}^A\text{Yb}(d,x){}^B\text{Lu}$  reaction together with their  $Q$ -values in units of MeV.

Activation product	$(d,p)$ & $(d,n)$ channels	$Q$ -value [MeV]	$(d,2n)$ channels	$Q$ -value [MeV]	$(d,3n)$ channels	$Q$ -value [MeV]	$(d,4n)$ channels	$Q$ -value [MeV]
${}^{177}\text{Lu}$	${}^{176}\text{Yb}(d,p)$	3.3						
${}^{176\text{m}}\text{Lu}$	${}^{176}\text{Yb}(d,n)$	4.0	${}^{176}\text{Yb}(d,2n)$	-3.1				
${}^{174\text{g}}\text{Lu}$			${}^{174}\text{Yb}(d,2n)$	-4.4			${}^{176}\text{Yb}(d,4n)$	-17.1
${}^{174\text{m}}\text{Lu}$	${}^{173}\text{Yb}(d,n)$	3.1	${}^{174}\text{Yb}(d,2n)$	-4.6			${}^{176}\text{Yb}(d,4n)$	-17.2
${}^{173}\text{Lu}$	${}^{173}\text{Yb}(d,n)$	3.3	${}^{173}\text{Yb}(d,2n)$	-3.7	${}^{174}\text{Yb}(d,3n)$	-11.1		
${}^{172}\text{Lu}$	${}^{172}\text{Yb}(d,n)$	2.7	${}^{172}\text{Yb}(d,2n)$	-5.5	${}^{173}\text{Yb}(d,3n)$	-11.9		
${}^{171}\text{Lu}$	${}^{171}\text{Yb}(d,n)$	2.5	${}^{171}\text{Yb}(d,2n)$	-4.5	${}^{172}\text{Yb}(d,3n)$	-12.5		
${}^{170}\text{Lu}$	${}^{170}\text{Yb}(d,n)$	2.1	${}^{170}\text{Yb}(d,2n)$	-6.5	${}^{171}\text{Yb}(d,3n)$	-13.1		
${}^{169}\text{Lu}$	${}^{168}\text{Yb}(d,n)$	1.6			${}^{170}\text{Yb}(d,3n)$	-13.8		

Here,  $\sigma_\alpha(E)$  is the excitation function of the individual reaction channel, and the  $f(E)$  is deuteron fluences in the  ${}^{\text{nat}}\text{Yb}$  sample that were obtained by performing the Particle and Heavy Ion Transport code System (PHITS)<sup>23</sup> simulation with the geometry of the experimental conditions discussed in Sect. 2. Note that the simulation code, such as the PHITS, is very useful for taking into account the attenuation of deuteron fluences in samples. Using the isotopic composition ratio of  ${}^A\text{Yb}$  present in  ${}^{\text{nat}}\text{Yb}$ ,  $R_A$ , the integral yield of  $Y({}^B\text{Lu})$  in the  ${}^{\text{nat}}\text{Yb}$  sample produced via the individual reaction channel,  $\alpha$ , is given by Eq. (2). Note that A is one of seven stable Yb isotopes of mass number 168, 170, 171, 172, 173, 174, and 176:

$$Y({}^B\text{Lu}) = \sum_A R_A \sum_{\alpha \in {}^B\text{Lu}} Y_\alpha. \quad (2)$$

Here,  $\alpha \in {}^B\text{Lu}$  means summation over all individual reaction channels  $\alpha$  contributing to produce the radionuclide  ${}^B\text{Lu}$ .  $Y({}^B\text{Lu})$  will be compared with the aforementioned measured integral yield of  ${}^B\text{Lu}$ , after we derive  $\sigma_\alpha(E_d)$  of the excitation function of the individual reaction channel,  $\alpha$ .

In the following discussion, the  $Q$ -value of the individual reaction channel,  $\alpha$ , plays an important role, and therefore we give all the  $Q$ -values of relevant reaction channels for producing  ${}^B\text{Lu}$  by the  ${}^A\text{Yb}(d,x){}^B\text{Lu}$  reaction at  $2 \leq E \leq 40$  MeV in Table III.

### 3.1 Method to determine excitation functions of individual reactions

#### 3.1.1 Excitation functions of the ${}^{176}\text{Yb}(d,x)$ reactions leading to produce ${}^{177}\text{Lu}$ and ${}^{176\text{m}}\text{Lu}$

Among reactions to produce a variety of Lu radionuclides by the  ${}^{\text{nat}}\text{Yb}(d,x)\text{Lu}$  reaction,  ${}^{177}\text{Lu}$  is produced by a cumulative sum of the indirect  ${}^{176}\text{Yb}(d,p){}^{177}\text{Yb} \rightarrow {}^{177}\text{Lu}$  and direct  ${}^{176}\text{Yb}(d,n){}^{177}\text{Lu}$  reactions, and  ${}^{176\text{m}}\text{Lu}$  is generated by the  ${}^{176}\text{Yb}(d,2n){}^{176\text{m}}\text{Lu}$  reaction. The unique identification of those reactions to produce  ${}^{177}\text{Lu}$  and  ${}^{176\text{m}}\text{Lu}$  comes from a fact that  ${}^{176}\text{Yb}$  is the heaviest stable isotope present in  ${}^{\text{nat}}\text{Yb}$ . Hence, those three reactions can be used to determine the excitation functions of the individual reactions to produce  ${}^{177}\text{Lu}$  and  ${}^{176\text{m}}\text{Lu}$ . Figure 2 shows the measured excitation functions for the  ${}^{176}\text{Yb}(d,p){}^{177}\text{Yb} \rightarrow {}^{177}\text{Lu}$ ,  ${}^{176}\text{Yb}(d,n){}^{177}\text{Lu}$ , and  ${}^{176}\text{Yb}(d,x){}^{177}\text{Lu}$  reactions which are denoted by closed squares, triangles, and circles, respectively. Note that the cross sections for the  ${}^{176}\text{Yb}(d,n){}^{177}\text{Lu}$  reaction at each incident deuteron energies were obtained by subtracting

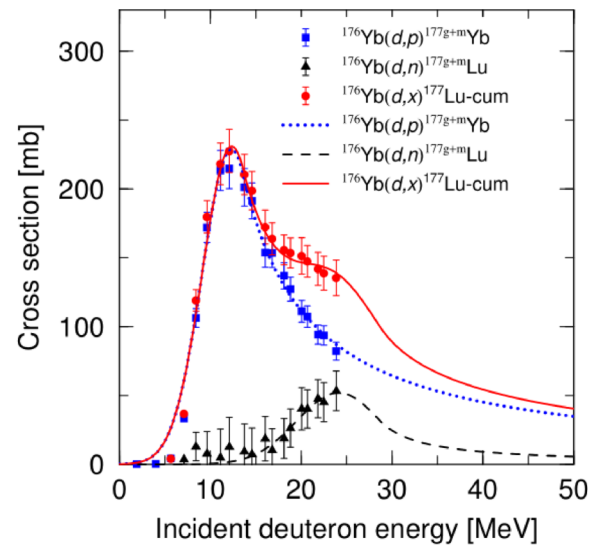


**Fig. 2.** (Color online) Measured excitation functions, taken from Khandaker et al.,<sup>16</sup> of the  ${}^{176}\text{Yb}(d,p){}^{177\text{g+m}}\text{Yb}$  (filled squares),  ${}^{176}\text{Yb}(d,n){}^{177\text{g+m}}\text{Lu}$  (filled triangle), and cumulative  ${}^{176}\text{Yb}(d,x){}^{177}\text{Lu}$  (filled circles) reactions. The fitted excitation functions of the reactions are shown by the solid, dotted and dashed lines.

those for the  ${}^{176}\text{Yb}(d,p){}^{177}\text{Yb} \rightarrow {}^{177}\text{Lu}$  reaction from those for the  ${}^{176}\text{Yb}(d,x){}^{177}\text{Lu}$  reaction.

The excitation functions of the individual  ${}^{176}\text{Yb}(d,p){}^{177}\text{Yb} \rightarrow {}^{177}\text{Lu}$  and  ${}^{176}\text{Yb}(d,n){}^{177}\text{Lu}$  reactions were obtained by fitting these measured excitation functions with a function that is given by Eq. (3) as the sum of a Gauss function at energies below  $E < E_{\text{sw}}$  and a reciprocal function at above  $E > E_{\text{sw}}$ :

$$\sigma_\alpha(E) = \begin{cases} a_1 \exp\left[-\frac{(E - a_2)^2}{(2a_3)^2}\right] & E < E_{\text{sw}}. \\ \frac{b_1}{E - b_2} & E_{\text{sw}} < E. \end{cases} \quad (3)$$

Here,  $E$  stands for the incident deuteron energy, and  $E_{\text{sw}}$  is the switching energy to connect the two functional types;  $a_i$  and  $b_j$  ( $i = 1, 2$ , and  $3$ ,  $j = 1$  and  $2$ ) are the parameters of the aforementioned functions. Two functions are smoothly connected by considering the continuity of the first derivative at  $E_{\text{sw}}$ . Note that  $a_1$  and  $a_2$  are the height of the Gaussian's peak and the energy of the center of the peak, and  $a_3$  is related to the full width at half maximum of the peak, respectively, and  $b_1$  and  $b_2$  are arbitrary constants that are

related to a normalization factor of the reciprocal function and the energy of the center of the peak. Here, it is worth mentioning that the excitation function of the  $^{176}\text{Yb}(d,2n)^{176\text{m}}\text{Lu}$  reaction was measured at a deuteron energy higher than the peak energy; that allowed us to determine the values of  $a_2$  and  $b_2$  by least-squares fits; their values are close to each other, 12.0 and 10.9, respectively. However, when excitation functions of the  $^{\text{nat}}\text{Yb}(d,x)^{\text{B}}\text{Lu}$  reaction have not yet been measured at deuteron energies higher than the peak cross section, values for  $a_2$  and  $b_2$  cannot be determined by least-squares fits. Therefore, in such a case two values were assumed to be identical to each other because they are related to the peak energy of the cross sections, as aforementioned. If excitation functions of the  $^{\text{nat}}\text{Yb}(d,x)^{\text{B}}\text{Lu}$  reaction are given to be composed of two reaction channels, such as the  $(d,2n)$  and  $(d,4n)$  reactions, the difference between the value for  $a_2$  (or  $b_2$ ) of the  $(d,2n)$  reaction and the value for  $a_2$  (or  $b_2$ ) of the  $(d,4n)$  reaction was assumed to be the same as the difference of the  $Q$ -value between the  $(d,2n)$  reaction and the  $(d,4n)$  reaction. Here, it is worth mentioning that the  $a_2$  value for the  $^{174}\text{Yb}(d,2n)^{174\text{g}+\text{m}}\text{Lu}$  reaction is 13.7 MeV and that for the  $^{176}\text{Yb}(d,4n)^{174\text{g}+\text{m}}\text{Lu}$  reaction is 26.4 MeV. The difference in their  $a_2$  values is 12.7 MeV, which is equal to the difference between the  $Q$ -value for the former reaction ( $-4.4$  MeV) and the  $Q$ -value for the latter reaction ( $-17.1$  MeV).

Using the function given by Eq. (3) the measured excitation functions for the  $^{176}\text{Yb}(d,p)^{177}\text{Yb} \rightarrow ^{177}\text{Lu}$ ,  $^{176}\text{Yb}(d,n)^{177}\text{Lu}$ , and  $^{176}\text{Yb}(d,x)^{177}\text{Lu}(\text{cum})$  reactions were fitted, as shown in Fig. 2. Here, although the excitation function of the  $^{176}\text{Yb}(d,n)^{177}\text{Lu}$  reaction has not yet been measured at a deuteron energy above 24 MeV, the peak energy, denoted by  $E_{\text{max}}$ , at which the cross section becomes maximal, was derived by fitting the measured cross sections with Eq. (3), resulting in  $E_{\text{max}} = 24$  MeV. This peak energy is about 12 MeV higher than that of the  $^{176}\text{Yb}(d,p)^{177}\text{Yb} \rightarrow ^{177}\text{Lu}$  reaction despite that the  $Q$ -value of the  $^{176}\text{Yb}(d,n)^{177}\text{Lu}$  reaction is only 0.6 MeV higher than that of the  $^{176}\text{Yb}(d,p)^{177}\text{Yb}$  reaction. The large difference between the peak energies was discussed by Hermanne et al. by considering the Coulomb barrier between Yb and the deuteron, which is about 13 MeV.<sup>15</sup> The peak energy of the  $(d,n)$  channel, therefore, is expected to be obtained by simply adding the Coulomb barrier energy of 13 to 12 MeV, the peak energy of the  $(d,p)$  reaction channel, and the result is consistent to the present estimation of  $E_{\text{max}} = 24$  MeV. Here, it should be noted that the  $(d,n)$  channel has a peak structure, because when the deuteron energy is as high as about 25 MeV, the  $(d,3n)$  reaction channel with a  $Q$ -value of  $-9.40$  MeV, leading to the stable  $^{175}\text{Lu}$  isotope, becomes dominant over the  $(d,n)$  reaction channel. Hence, the cross section of the  $(d,n)$  channel decreases with increasing the deuteron energy, resulting in the peak structure for the  $(d,n)$  reaction channel. The excitation function of the  $^{176}\text{Yb}(d,n)^{177}\text{Lu}$  reaction above  $E > 25$  MeV remains to be measured for testing the estimated shape. In this study, we obtained the three parameters  $a_i$  ( $i = 1, 2,$  and  $3$ ) in Eq. (3) for the  $^{176}\text{Yb}(d,n)^{177}\text{Lu}$  reaction by the fitting procedure, and then determined  $b_1$  and  $E_{\text{sw}}$  so as to smoothly connect the two fitting functions, assuming that  $a_2$  and  $b_2$  are equal.

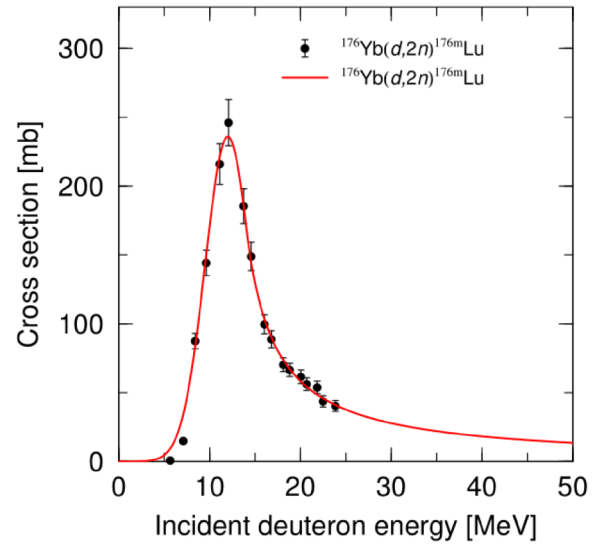
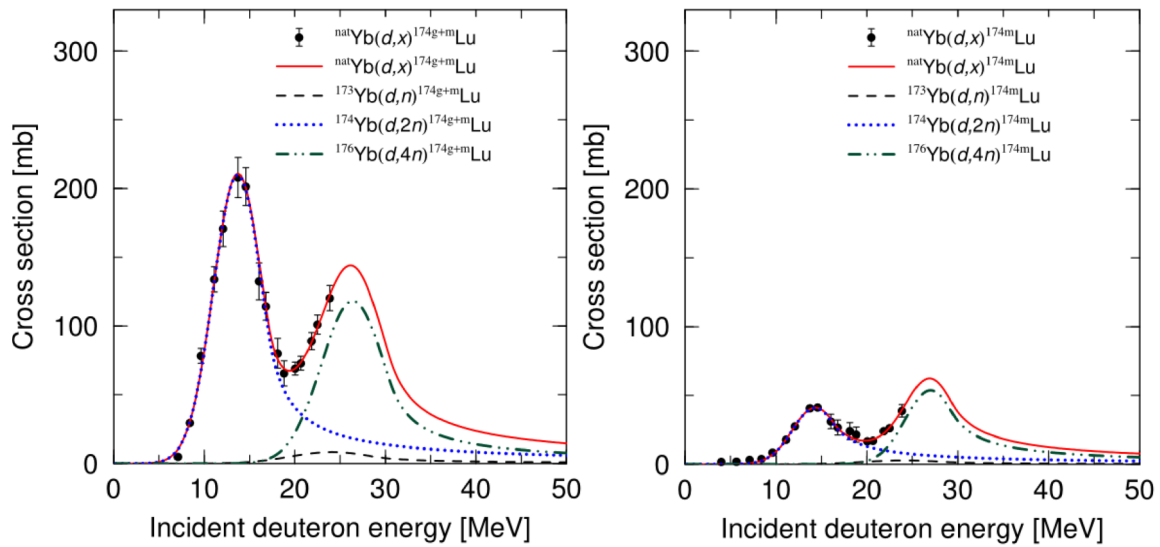


Fig. 3. (Color online) Measured<sup>16)</sup> and fitted excitation functions of the  $^{176}\text{Yb}(d,2n)^{176\text{m}}\text{Lu}$  reaction.

Similarly, the measured excitation function of the  $^{176}\text{Yb}(d,2n)^{176\text{m}}\text{Lu}$  reaction was fitted with Eq. (3), as shown in Fig. 3. Note that the deuteron energy,  $E_{\text{max}}$ , of the reaction is about 11.7 MeV, which is 8.6 MeV higher than the  $Q$ -value of  $-3.1$  MeV. Hence, we used Eq. (3) to fit all of the data in the following discussions.

### 3.1.2 Excitation function for cumulative productions of Lu radionuclides by the $^{\text{nat}}\text{Yb}(d,x)\text{Lu}$ reaction

We discuss an excitation function for cumulative productions of  $^{\text{B}}\text{Lu}$  by the  $^{\text{nat}}\text{Yb}(d,x)^{\text{B}}\text{Lu}$  reaction.  $^{174\text{g}}\text{Lu}$  ( $T_{1/2} = 3.31$  y) is cumulatively produced by the  $^{173}\text{Yb}(d,n)$ ,  $^{174}\text{Yb}(d,2n)$ , and  $^{176}\text{Yb}(d,4n)$  reactions, and an isomeric decay of the isomeric state at 171 keV ( $T_{1/2} = 142$  d).<sup>13–16</sup> In fact, in the measured excitation function of the  $^{\text{nat}}\text{Yb}(d,x)^{174\text{g}+\text{m}}\text{Lu}$  reaction shown in the left panel of Fig. 4 (filled circle), we can clearly see the two peaks at about 14 and 26 MeV contributing  $^{174\text{g}+\text{m}}\text{Lu}$  yields that result from two different nuclear reactions. These reactions are  $^{174}\text{Yb}(d,2n)^{174\text{g}+\text{m}}\text{Lu}$  and  $^{176}\text{Yb}(d,4n)^{174\text{g}+\text{m}}\text{Lu}$  from the  $Q$ -values of their reactions, as listed in Table III. The measured excitation function of the  $^{\text{nat}}\text{Yb}(d,x)^{174\text{g}+\text{m}}\text{Lu}$  reaction was fitted using Eq. (3), as shown in the left panel of Fig. 4 (solid line), by considering the isotopic compositions of Yb in the  $^{\text{nat}}\text{Yb}$  sample. The peak deuteron energy,  $E_{\text{max}}$ , of the  $^{\text{nat}}\text{Yb}(d,x)^{174\text{g}+\text{m}}\text{Lu}$  reaction is about 14 and 9.6 MeV higher than the threshold energy of the  $^{174}\text{Yb}(d,2n)^{174\text{g}}\text{Lu}$  reaction, suggesting that the maximum cross section is dominated by this reaction. As for the second peak at about 24 MeV, we note that the measured cross section of the  $^{\text{nat}}\text{Yb}(d,x)^{174\text{g}+\text{m}}\text{Lu}$  reaction at  $E \geq 20$  MeV goes up with increasing deuteron energy, and conclude that the peak is most likely to be due to the  $^{176}\text{Yb}(d,4n)^{174\text{g}+\text{m}}\text{Lu}$  reaction. In addition, the  $^{173}\text{Yb}(d,n)^{174\text{g}+\text{m}}\text{Lu}$  reaction might also contribute to the measured yield of  $^{174\text{g}+\text{m}}\text{Lu}$ , similarly to the case of the  $^{176}\text{Yb}(d,n)^{177}\text{Lu}$  reaction. Here, because the excitation function of the  $^{173}\text{Yb}(d,n)^{174\text{g}+\text{m}}\text{Lu}$  reaction as well as  $E_{\text{max}}$  has not yet been measured at  $E = 2\text{--}40$  MeV, they were assumed to be the same as those of the  $^{176}\text{Yb}(d,n)^{177}\text{Lu}$  reaction. We determined the fitting parameters including  $a_2$



**Fig. 4.** (Color online) Measured<sup>16)</sup> (filled circles) and fitted (solid, dotted, and dashed lines) excitation function of the  ${}^{\text{nat}}\text{Yb}(d,x){}^{174\text{g+m}}\text{Lu}$  (left) and  ${}^{\text{nat}}\text{Yb}(d,x){}^{174\text{m}}\text{Lu}$  (right) reactions.

and  $b_2$  for the  ${}^{174}\text{Yb}(d,2n){}^{174\text{g+m}}\text{Lu}$  reaction by the least-squares method so as to reproduce the peak structure at  $E$  of around 14 MeV. Then, the parameters of the excitation function for the  ${}^{176}\text{Yb}(d,4n){}^{174\text{g+m}}\text{Lu}$  reaction were determined by using the measured data at  $E \geq 20$  MeV after subtracting the yields of the  ${}^{173}\text{Yb}(d,n){}^{174\text{g+m}}\text{Lu}$  and  ${}^{174}\text{Yb}(d,2n){}^{174\text{g+m}}\text{Lu}$  reactions. In the fit, we assumed the parameters  $a_2 = 26.4$  and  $b_2 = 27.6$  for the  ${}^{176}\text{Yb}(d,4n){}^{174\text{g+m}}\text{Lu}$  reaction, which were obtained by adding the difference of  $Q$ -value, 12.7, to the values for  $a_2$  and  $b_2$  for the  ${}^{174}\text{Yb}(d,2n){}^{174\text{g+m}}\text{Lu}$  reaction. Similarly, the measured excitation function of the  ${}^{\text{nat}}\text{Yb}(d,x){}^{174\text{m}}\text{Lu}$  reaction was fitted using Eq. (3), as shown in the right panel of Fig. 4.

Secondly, we note a measured excitation function of the  ${}^{\text{nat}}\text{Yb}(d,x){}^{173}\text{Lu}$  reaction with one broad peak, as shown in Fig. 5. The excitation function was fitted by employing Eq. (3) while taking into account the isotopic compositions of Yb in the  ${}^{\text{nat}}\text{Yb}$  sample. It turned out that the  ${}^{172}\text{Yb}(d,n){}^{173}\text{Lu}$ ,  ${}^{173}\text{Yb}(d,2n){}^{173}\text{Lu}$ , and  ${}^{174}\text{Yb}(d,3n){}^{173}\text{Lu}$  reactions predominantly contribute to form the measured excitation function. Here, we assumed that the excitation function of the  ${}^{176}\text{Yb}(d,n){}^{177}\text{Lu}$  reaction is the same as that of the  ${}^{172}\text{Yb}(d,n){}^{173}\text{Lu}$  reaction with a  $Q$ -value of 2.7 MeV. After subtracting the yield of the  ${}^{172}\text{Yb}(d,n){}^{173}\text{Lu}$  reaction using the measured excitation function of the  ${}^{\text{nat}}\text{Yb}(d,x){}^{173}\text{Lu}$  reaction, we performed the fit procedure mentioned above to determine the parameters of the excitation function of the  ${}^{173}\text{Yb}(d,2n){}^{173}\text{Lu}$  and  ${}^{174}\text{Yb}(d,3n){}^{173}\text{Lu}$  reactions. Here, we assumed that the value of the parameter  $a_2$  is equal to that of  $b_2$  for both reactions.

Similarly, the measured excitation functions of the  ${}^{\text{nat}}\text{Yb}(d,x){}^{172\text{g+m}}\text{Lu}$ ,  ${}^{\text{nat}}\text{Yb}(d,x){}^{171\text{g+m}}\text{Lu}$ ,  ${}^{\text{nat}}\text{Yb}(d,x){}^{170\text{g+m}}\text{Lu}$ , and  ${}^{\text{nat}}\text{Yb}(d,x){}^{169\text{g+m}}\text{Lu}$  reactions were also fitted using Eq. (3), as shown in Fig. 6. Here,  ${}^{169\text{g+m}}\text{Lu}$  is considered to be mainly produced by the  ${}^{170}\text{Yb}(d,3n){}^{169\text{g+m}}\text{Lu}$  reaction by noting the isotopic compositions for  ${}^{168}\text{Yb}$  and  ${}^{170}\text{Yb}$  are 0.1 and 3.0%, respectively.

Through the least-squares fit of the measured excitation functions of a variety of Lu radionuclides produced by the  ${}^{\text{nat}}\text{Yb}(d,x)\text{Lu}$  reaction using Eq. (3), we obtained values of all

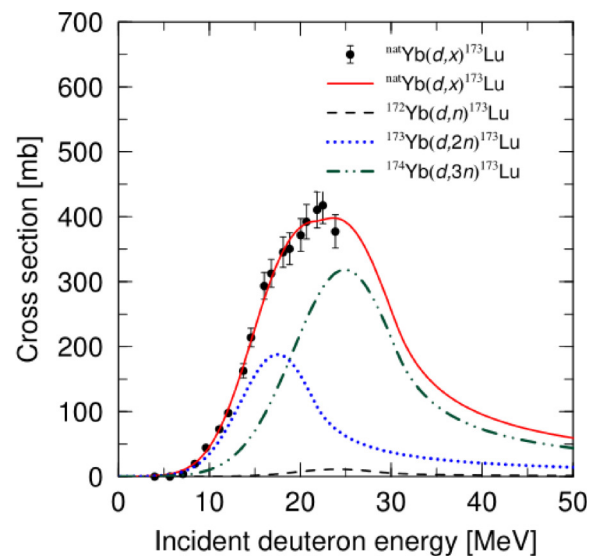


**Fig. 5.** (Color online) Measured<sup>16)</sup> (filled circles) and fitted (several lines) excitation function for the  ${}^{\text{nat}}\text{Yb}(d,x){}^{173}\text{Lu}$  reaction.

parameters ( $a_1$ ,  $a_2$ ,  $a_3$ ,  $b_1$ ,  $b_2$ , and  $E_{\text{sw}}$ ) as listed in Table IV. Namely, we obtained excitation functions of individual reactions to calculate production yields of Lu radionuclides using enriched  ${}^{176}\text{Yb}$  samples having a variety of isotopic compositions of Yb.

## 4. Results

### 4.1 Comparison of the measured and calculated integral yields of Lu radionuclides

We tested the validity of the excitation functions of the individual reactions that were derived in the previous section, as follows. We first calculated the integral yields of Lu radionuclides at the EOI that will be generated by irradiating a  ${}^{\text{nat}}\text{Yb}$  sample with 25 MeV deuteron beams, and compared them with the measured integral yields. The calculations were undertaken using the aforementioned excitation functions of individual reactions, the isotopic compositions of  ${}^{\text{nat}}\text{Yb}$ , and the deuteron-fluences in the  ${}^{\text{nat}}\text{Yb}$  sample,  $f(E)$ . The fluences,  $f(E)$ , were obtained by performing a particle transport

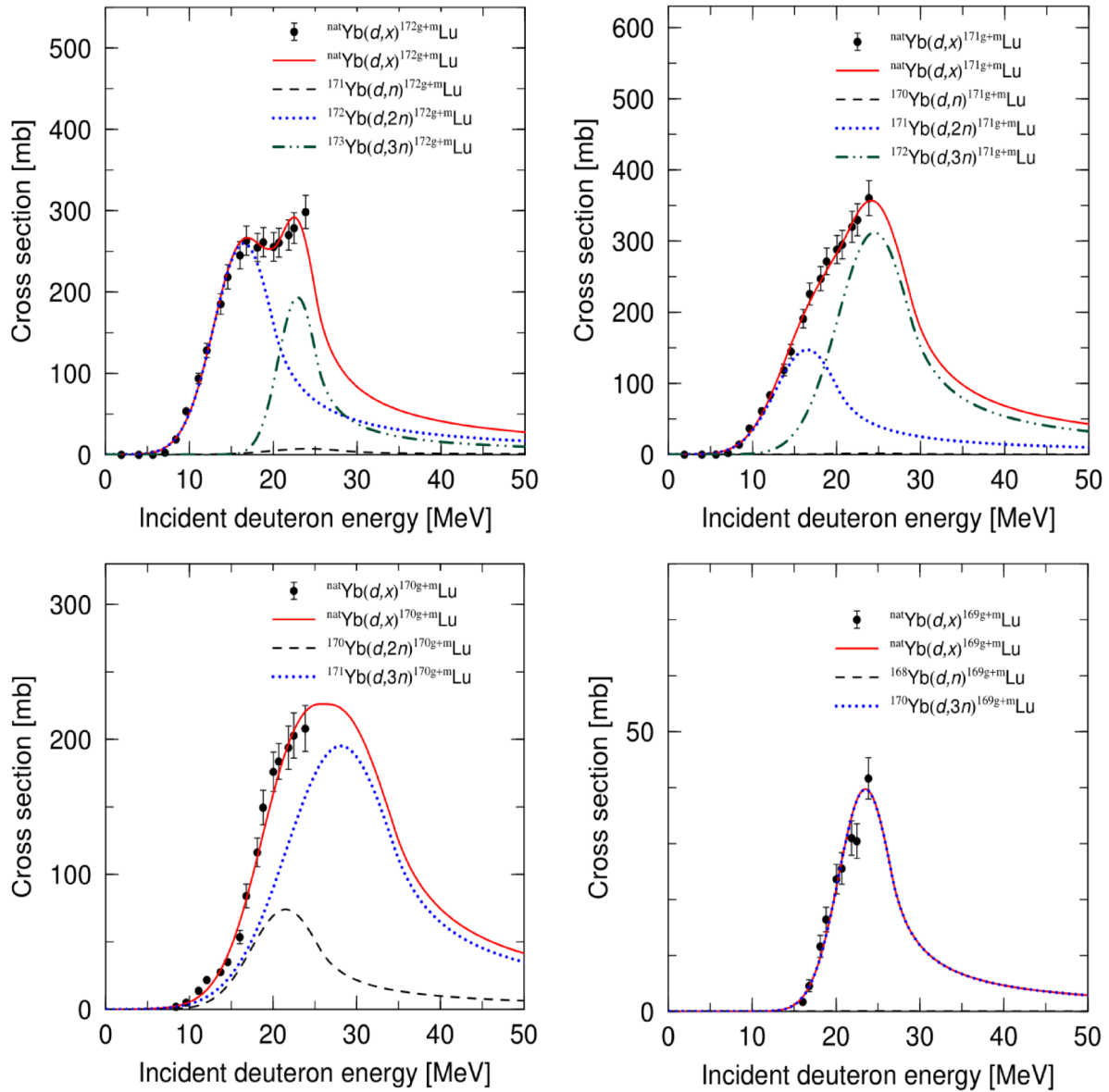


**Fig. 6.** (Color online) Measured<sup>16)</sup> and fitted excitation functions for the  ${}^{\text{nat}}\text{Yb}(d,x){}^{172\text{g}+\text{m}}\text{Lu}$  (upper-left),  ${}^{\text{nat}}\text{Yb}(d,x){}^{171\text{g}+\text{m}}\text{Lu}$  (upper-right),  ${}^{\text{nat}}\text{Yb}(d,x){}^{170\text{g}+\text{m}}\text{Lu}$  (lower-left), and  ${}^{\text{nat}}\text{Yb}(d,x){}^{169\text{g}+\text{m}}\text{Lu}$  (lower-right) reactions.

**Table IV.** Obtained values of all parameters given in Eq. (3) and  $Q$ -values in units of MeV.

	$Q$ -value	$a_1$	$a_2$	$a_3$	$b_1$	$b_2$	$E_{\text{sw}}$
${}^{176}\text{Yb}(d,p){}^{177\text{g}+\text{m}}\text{Yb}$	3.3	229	12.3	3.2	1519	6.4	13.7
${}^{176}\text{Yb}(d,n){}^{177}\text{Lu}$	4.0	52	24.1	4.6	145	24.1	28.7
${}^{176}\text{Yb}(d,2n){}^{176\text{m}}\text{Lu}$	-3.1	236	12.0	2.5	531	10.9	14.0
${}^{174}\text{Yb}(d,2n){}^{174\text{m}}\text{Lu}$	-4.6	128	14.3	2.5	270	13.4	16.4
${}^{174}\text{Yb}(d,2n){}^{174\text{g}+\text{m}}\text{Lu}$	-4.4	655	13.7	2.7	652	14.9	17.1
${}^{176}\text{Yb}(d,4n){}^{174\text{m}}\text{Lu}$	-17.2	413	27.0	2.8	944	26.1	29.4
${}^{176}\text{Yb}(d,4n){}^{174\text{g}+\text{m}}\text{Lu}$	-17.1	910	26.4	3.5	1329	27.6	30.6
${}^{173}\text{Yb}(d,2n){}^{173}\text{Lu}$	-3.7	1167	17.5	4.1	2902	17.5	21.6
${}^{174}\text{Yb}(d,3n){}^{173}\text{Lu}$	-11.1	994	24.9	5.7	3436	24.9	30.6
${}^{172}\text{Yb}(d,2n){}^{172\text{g}+\text{m}}\text{Lu}$	-5.5	1198	16.5	3.6	2616	16.5	20.1
${}^{173}\text{Yb}(d,3n){}^{172\text{g}+\text{m}}\text{Lu}$	-11.9	1201	22.9	2.3	1675	22.9	25.2
${}^{171}\text{Yb}(d,2n){}^{171\text{g}+\text{m}}\text{Lu}$	-4.5	1046	16.5	3.8	2411	16.5	20.3
${}^{172}\text{Yb}(d,3n){}^{171\text{g}+\text{m}}\text{Lu}$	-12.5	1439	24.5	4.4	3840	24.5	28.9
${}^{170}\text{Yb}(d,2n){}^{170\text{g}+\text{m}}\text{Lu}$	-6.5	2486	21.5	4.1	6182	21.5	25.6
${}^{171}\text{Yb}(d,3n){}^{170\text{g}+\text{m}}\text{Lu}$	-13.1	1385	28.1	6.5	5460	28.1	34.6
${}^{170}\text{Yb}(d,3n){}^{169\text{g}+\text{m}}\text{Lu}$	-13.8	1332	23.5	3.2	2585	23.5	26.7

simulation using the PHITS code while taking into account the geometry of the experimental setup, discussed in Sect. 2. The intensity of the deuteron beam irradiated on the  ${}^{\text{nat}}\text{Yb}$  sample as well as the deuteron beam irradiation time was the same as that of the present measurement. Here, we summed over all reaction channels that contributed to produce a radionuclide  ${}^{\text{B}}\text{Lu}$ , as given by Eq. (2).

The calculated integral yields of Lu radionuclides are in good agreement mostly with the measured yields within the experimental uncertainties, as shown in Table V. Here, the total systematic uncertainties in the calculation were evaluated to be 14% by considering errors associated with the total uncertainty of the data (12.8%) by Khandaker et al.<sup>16)</sup> and parameters (5%) that were used in the fit. The total uncertainty of the measured yield was estimated to be 12%, as aforementioned. The agreement clearly suggests that the fitted approach for the individual reactions presented in the last section can be used to estimate the yields of Lu radionuclides, i.e., the radionuclide purity of  ${}^{177}\text{Lu}$ , which will be produced by irradiating an enriched  ${}^{176}\text{Yb}$  sample

**Table V.** Calculated integral yields of Lu radionuclides at the EOI that will be generated by irradiating a <sup>nat</sup>Yb sample with 25 MeV deuteron beams are compared with the measured ones. Here, <sup>174g</sup>Lu ( $T_{1/2} = 3.31$  y) should be noted to be produced not only by the <sup>173</sup>Yb(*d,n*), <sup>174</sup>Yb(*d,2n*), and <sup>176</sup>Yb(*d,4n*) reactions but also from an isomeric decay of the isomeric state at 171 keV of <sup>174m</sup>Lu ( $T_{1/2} = 142$  d). Since in this study, the yield of <sup>174g</sup>Lu was measured 37 days after the EOI, it is compared to the calculated yield corresponding to the yield at 37 days after the EOI.

Nucleide	$T_{1/2}$	$E_\gamma$ (keV)	Yield (Bq)	
			Meas.	Cal.
<sup>177g</sup> Lu	6.65 d	208.4	8.61E+04	8.83E+04
<sup>176m</sup> Lu	3.66 h	88.4	1.36E+06	2.41E+06
<sup>174g</sup> Lu	3.31 y	1241.8	2.21E+03	2.02E+03
<sup>173</sup> Lu	1.37 y	272.1	1.56E+04	1.49E+04
<sup>172g</sup> Lu	6.70 d	900.7	8.23E+05	8.93E+05
<sup>171g</sup> Lu	8.24 d	739.8	8.96E+05	7.23E+05
<sup>170g</sup> Lu	2.0 d	1280.3	1.13E+06	1.48E+06
<sup>169g</sup> Lu	34.1 h	191.2	2.68E+05	2.95E+05

having a variety of isotopic compositions of Yb. Consequently, we can estimate the radionuclide purity of <sup>177</sup>Lu as a function of the deuteron energy. Note that the yield of <sup>174m</sup>Lu was not obtained because low energy  $\gamma$ -rays, such as 44 and 67 keV  $\gamma$ -rays, were not clearly identified in this study, and the yield of <sup>177m</sup>Lu ( $T_{1/2} = 160.4$  d) derived by analyzing the 367.4 keV  $\gamma$ -ray line ( $I_\gamma = 52.4\%$ ) of <sup>177m</sup>Lu is less than 1/100 of that of <sup>177</sup>Lu.

#### 4.2 Isotopic compositions of Yb in enriched <sup>176</sup>Yb samples and radionuclide purity of <sup>177</sup>Lu

On the basis of the reasonable agreement between the calculated integral yields of Lu radionuclides and the measured ones, we estimated the yields of Lu radionuclides that will be produced by irradiating enriched <sup>176</sup>Yb samples having three sets of the isotopic compositions of Yb (discussed below) with deuteron beams. Here, the excitation functions of individual reactions given in Table IV and the PHITS code were used, and the deuteron energies were 15, 20, and 25 MeV.

##### 4.2.1 Yields of Lu radionuclides for a Yb sample of 100% enriched in <sup>176</sup>Yb

We first estimated the yields of impurity radionuclides of Lu produced by using a 100% enriched <sup>176</sup>Yb sample. The study provides information on the deuteron energy dependence of the yields of impurity radionuclides of <sup>174g+m</sup>Lu (<sup>174g</sup>Lu/<sup>177</sup>Lu + <sup>174m</sup>Lu/<sup>177</sup>Lu) and <sup>176m</sup>Lu. The estimated results are given in Table VI; the activity ratio of <sup>174g+m</sup>Lu/<sup>177</sup>Lu drops down significantly with decreasing deuteron energy, that is 0.019, 0.0013, and 0.00 at  $E = 25, 20,$  and 15 MeV, and that of <sup>176m</sup>Lu/<sup>177</sup>Lu at the EOI is large: 39, 32, and 27 at  $E = 15, 20,$  and 25 MeV. Here, it should be noted that the activity ratio, <sup>176m</sup>Lu/<sup>177</sup>Lu, at 2.5 days after the EOI is significantly reduced by about 1/10<sup>5</sup> because the half-life of <sup>176m</sup>Lu ( $T_{1/2} = 3.64$  h) is shorter than that of <sup>177</sup>Lu ( $T_{1/2} = 6.65$  d), although there is a 23% loss of the <sup>177</sup>Lu activity. A separation of Lu radionuclides from irradiated Yb samples necessary to obtain carrier-free <sup>177</sup>Lu can be done within two days after the EOI. Here, it should be mentioned that the integral yields of <sup>177</sup>Lu at  $E = 15$  and 20 MeV are, respectively, reduced by 60 and 30% of that at  $E = 25$  MeV.

**Table VI.** Estimated activity ratio of <sup>174g+m</sup>Lu and <sup>176m</sup>Lu to <sup>177</sup>Lu at the EOI and 2.5 days after the EOI at  $E = 15, 20,$  and 25 MeV in the case of a 100% enriched <sup>176</sup>Yb sample. The activity of <sup>177</sup>Lu at a deuteron energy of 25 MeV is normalized to 1.0.

Activity ratio	Deuteron energy		
	15 MeV	20 MeV	25 MeV
<sup>B</sup> Lu/ <sup>177g</sup> Lu			
<sup>174m</sup> Lu/ <sup>177g</sup> Lu (EOI)	0	0.0005	0.014
<sup>174g</sup> Lu/ <sup>177g</sup> Lu (EOI)	0	0.0008	0.0049
<sup>176m</sup> Lu/ <sup>177g</sup> Lu (EOI)	39	32	27
<sup>176m</sup> Lu/ <sup>177g</sup> Lu (2.5 days after EOI)	0.0009	0.0008	0.0006
<sup>177g</sup> Lu activity vs deuteron energy	0.4	0.7	1

##### 4.2.2 Yields of Lu radionuclides for enriched <sup>176</sup>Yb samples with several isotopic compositions of Yb

Next, we estimated the activity ratio of <sup>B</sup>Lu to <sup>177</sup>Lu (<sup>B</sup>Lu/<sup>177</sup>Lu) for <sup>A</sup>Yb present in 99.90 and 97.6% enriched <sup>176</sup>Yb samples at 2.5 days after the EOI when 99.90 and 97.6% enriched <sup>176</sup>Yb samples are irradiated with deuterons of 15, 20, and 25 MeV. These samples are commercially available from TRACE SCIENCES INTERNATIONAL and ISOFLEX USA, respectively. The isotopic compositions of <sup>A</sup>Yb in 99.90 and 97.6% (in brackets) enriched <sup>176</sup>Yb samples and estimated activity ratio are given in Table VII.

In order to obtain <sup>177</sup>Lu with high radionuclide purity we discuss the origins of each impurity of the Lu radionuclide and its deuteron energy dependence in the following. Firstly, the present results demonstrate that a significant amount of <sup>177</sup>Lu with a radionuclide impurity of less than a few% can be produced by irradiating commercially available enriched <sup>176</sup>Yb samples with deuteron beams at  $15 \leq E \leq 25$  MeV. The radionuclide purity of <sup>177</sup>Lu for the 99.90% (97.60%) enriched <sup>176</sup>Yb samples at 2.5 days after the EOI is >95% (>95%), >99% (98%), and >99% (99%) at  $E = 25, 20,$  and 15 MeV. Secondly, the yield of <sup>174m</sup>Lu as well as those of <sup>177</sup>Lu and <sup>176m</sup>Lu are almost the same for two enriched <sup>176</sup>Yb samples. Note that both <sup>177</sup>Lu and <sup>176m</sup>Lu are produced by the <sup>176</sup>Yb(*d,x*)<sup>177</sup>Lu and <sup>176</sup>Yb(*d,2n*)<sup>176m</sup>Lu reactions, as given in Table III. Hence, <sup>174g+m</sup>Lu is considered to be mainly produced by the <sup>176</sup>Yb(*d,4n*)<sup>174g+m</sup>Lu reaction but not the <sup>174</sup>Yb(*d,2n*)<sup>174g+m</sup>Lu and <sup>173</sup>Yb(*d,n*)<sup>174g+m</sup>Lu reactions. This finding is very important because the yield of <sup>174m</sup>Lu can be controlled by the deuteron energy. For example, the estimated activity ratio <sup>174m</sup>Lu/<sup>177</sup>Lu decreases significantly from 0.018 to 0.0005 by changing the deuteron energy from 25 to 20 MeV, although the yield of <sup>177</sup>Lu decreases by 30%. Thirdly, <sup>173</sup>Lu is mainly generated by the <sup>173</sup>Yb(*d,2n*)<sup>173</sup>Lu reaction, but not the <sup>174</sup>Yb(*d,3n*)<sup>173</sup>Lu reaction. Namely, the isotopic compositions of <sup>174</sup>Yb in enriched <sup>176</sup>Yb samples do not reduce the radionuclide purity of <sup>177</sup>Lu. This fact is an important finding for preparing enriched <sup>176</sup>Yb samples because the isotopic compositions of Yb in enriched <sup>176</sup>Yb samples generally drops down with decreasing the mass number of Yb. For example, in the case of 97.6% enriched <sup>176</sup>Yb sample shown in brackets in Table VII, the ratio of the isotopic composition of <sup>A</sup>Yb present in <sup>176</sup>Yb to the isotopic composition of <sup>A</sup>Yb present in <sup>nat</sup>Yb is 1.93/32.0 = 0.06 for A = 174. It is 0.011 for <sup>173</sup>Yb, 0.010 for A = 172, 0.005 for A = 171 and less than 0.003 for A = 170. Fourthly, the main production routes for <sup>172</sup>Lu, <sup>170</sup>Lu, and <sup>169</sup>Lu are the <sup>172</sup>Yb(*d,2n*)<sup>172g+m</sup>Lu reaction, the <sup>170</sup>Yb(*d,2n*)<sup>170g+m</sup>Lu reac-

**Table VII.** The isotopic composition of  $^{A}\text{Yb}$  in 99.90 and 97.6% (in brackets) enriched  $^{176}\text{Yb}$  sample and estimated activity ratio of  $^{B}\text{Lu}$  to  $^{177}\text{Lu}$  ( $\text{Lu}/^{177}\text{Lu}$ ) when the  $^{176}\text{Yb}$  samples at 2.5 days after the EOI are irradiated with deuterons of 15, 20, and 25 MeV. The sum of the activity ratio ( $^{\text{sum}}\text{Lu}/^{177}\text{Lu}$ ) is also shown, where  $^{\text{sum}}\text{Lu}$  is the total activity of produced Lu other than  $^{177}\text{Lu}$ . The activity of  $^{177}\text{Lu}$  at a deuteron energy of 25 MeV is normalized to 1.0.

$^{A}\text{Yb}$	Isotopic composition ratio $^{A}\text{Yb}/^{176}\text{Yb}$	Activity ratio $^{B}\text{Lu}/^{177}\text{Lu}$	Deuteron energy		
			15 MeV	20 MeV	25 MeV
$^{168}\text{Yb}$	<0.05 (<0.01)	$^{169}\text{gLu}/^{177}\text{Lu}$	<0.0000 (0.0000)	<0.0008 (<0.0002)	<0.0028 (<0.0006)
$^{170}\text{Yb}$	<0.05 (<0.01)	$^{170}\text{gLu}/^{177}\text{Lu}$	<0.0013 (<0.0007)	<0.0005 (<0.0025)	<0.0099 (<0.0053)
$^{171}\text{Yb}$	<0.05 (0.07)	$^{171}\text{gLu}/^{177}\text{Lu}$	<0.0016 (0.0019)	<0.0022 (0.0048)	<0.0032 (0.0090)
$^{172}\text{Yb}$	<0.05 (0.22)	$^{172}\text{gLu}/^{177}\text{Lu}$	<0.0012 (0.0059)	<0.0024 (0.011)	<0.0033 (0.014)
$^{173}\text{Yb}$	<0.05 (0.18)	$^{173}\text{Lu}/^{177}\text{Lu}$	0.0000 (0.0003)	0.0000 (0.0006)	<0.0001 (0.0012)
$^{174}\text{Yb}$	0.08 (1.93)	$^{174\text{m}}\text{Lu}/^{177}\text{Lu}$	0.0000 (0.0004)	0.0005 (0.0010)	0.018 (0.019)
		$^{174\text{g}}\text{Lu}/^{177}\text{Lu}$	0.0000 (0.0003)	0.0010 (0.0012)	0.0064 (0.0065)
$^{176}\text{Yb}$	99.90 (97.60)	$^{176\text{m}}\text{Lu}/^{177}\text{Lu}$	0.0009 (0.0009)	0.0008 (0.0008)	0.0006 (0.0006)
		$^{\text{sum}}\text{Lu}/^{177}\text{Lu}$	0.005 (0.010)	0.008 (0.022)	0.044 (0.052)
		$^{177}\text{Lu}$ activity vs deuteron energy	0.40 (0.40)	0.70 (0.70)	1.0 (1.0)

tion and the  $^{170}\text{Yb}(d,3n)^{169\text{g+m}}\text{Lu}$  reaction, respectively. However,  $^{171}\text{gLu}$  is generated by both the  $^{171}\text{Yb}(d,2n)^{171\text{g+m}}\text{Lu}$  and  $^{172}\text{Yb}(d,3n)^{171\text{g+m}}\text{Lu}$  reactions.

### 5. Summary

We developed a method for estimating the isotopic compositions of enriched  $^{176}\text{Yb}$  samples required to produce a carrier-free  $^{177}\text{Lu}$  with high radionuclide purity by the  $^{176}\text{Yb}(d,x)^{177}\text{Lu}$  reaction. Here, we derived the excitation function of individual reactions for producing a radionuclide of  $^{B}\text{Lu}$ , such as  $^{169}\text{Lu}$ ,  $^{170}\text{Lu}$ ,  $^{171}\text{Lu}$ ,  $^{172}\text{Lu}$ ,  $^{173}\text{Lu}$ ,  $^{174\text{g}}\text{Lu}$ ,  $^{174\text{m}}\text{Lu}$ ,  $^{176\text{m}}\text{Lu}$ , and  $^{177}\text{Lu}$ , using the latest measured excitation functions of the  $^{\text{nat}}\text{Yb}(d,x)\text{Lu}$  reactions. Note that we demonstrated that our measured integral yields of a variety of Lu radionuclides produced by the  $^{\text{nat}}\text{Yb}(d,x)\text{Lu}$  reaction agree with the calculated integral yields of Lu radionuclides using the derived excitation functions. Our results demonstrate that the estimated radionuclide purity of  $^{177}\text{Lu}$  for the 99.90 and 97.60% enriched  $^{176}\text{Yb}$  samples at 2.5 days after the EOI is >98 and >99% at  $E = 20$  and 15 MeV. We also evaluated an integral yield of the carrier-free  $^{177}\text{Lu}$  that is obtained by irradiating a  $^{176}\text{Yb}$  sample of 0.25 mm thickness with a 100  $\mu\text{A}$ , 25 MeV deuteron beams for 24 h. The yield is calculated to be 28 GBq using the measure yield of  $^{177}\text{Lu}$ ,  $8.61 \times 10^4$  Bq as given in Table II, that was obtained by irradiating the thick  $^{\text{nat}}\text{Yb}$  sample (the abundance of  $^{176}\text{Yb}$  is 13.0%) with 0.338  $\mu\text{A}$  deuteron beams for 10 min. This yield is compared with a typical carrier-free  $^{177}\text{Lu}$  activity of about 8 GBq; that is produced in a reactor with a typical thermal neutron flux of  $1.0 \times 10^{14}$  n/cm<sup>2</sup>/sec for a neutron irradiation time of 24 h using an enriched  $^{176}\text{Yb}$  sample of 100 mg.<sup>24)</sup> Here, we note a typical dose of therapeutic radiation of  $^{177}\text{Lu}$ -radiopharmaceuticals that is delivered to tumor cells. Lu-177 dotatate (Lutathera<sup>®</sup>) was approved by the U.S. Food and Drug Administration (FDA) in 2018 (in the EU approved by the European Medicines Agency in 2017) for the treatment of neuroendocrine tumors that occur in the gastrointestinal tract, such as stomach, small and large intestine, pancreas and appendix, and lungs. The recommended dosage of  $^{177}\text{Lu}$ -dotatate by the FDA is 7.4 GBq/patient every 8 weeks four intravenous infusions.<sup>22)</sup> Therefore, the present yield of 28 GBq/day encourages us to produce  $^{177}\text{Lu}$  by the  $^{176}\text{Yb}(d,x)^{177}\text{Lu}$  reaction using enriched  $^{176}\text{Yb}$  samples. The production method of  $^{177}\text{Lu}$  by the  $^{176}\text{Yb}(d,x)^{177}\text{Lu}$  reaction will play an important role in

promoting the widespread use of  $^{177}\text{Lu}$  for a variety of therapeutic applications. In addition, the present method would play an important role in determining the isotopic compositions of enriched samples for producing medical radionuclides with high radionuclide purity from measured excitation functions of nuclear reactions of natural samples in accelerators.

**Acknowledgments** We thank H. Haba for useful discussion and Y. Kawachi, Y. Koguchi, and T. Shibata for their continuous support and the operating crew of the CYRIC Cyclotron for ensuring reliable operation of the equipment. The present work was supported in part by JSPS KAKENHI Grant Numbers JP16K05383, JP19K03903, JP19K08163, and in part by Program on Open Innovation Platform with Enterprises, Research Institute and Academia, Japan Science and Technology Agency (JST, OPERA, JPMJOP1721).

- 1) D. Ersahin, I. Doddamane, and D. Cheng, *Cancers* **3**, 3838 (2011).
- 2) S. C. Srivastava and L. F. Mausner, Therapeutic Radionuclides: Production, Physical Characteristics, and Applications in *Therapeutic Nuclear Medicine, Medical Radiology, Radiation Oncology*, ed. R. P. Baum (Springer, Berlin/Heidelberg, 2013) p. 11.
- 3) C. S. Cutler, H. M. Hennkens, S. Sisay, S. Huclier-Markai, and S. S. Jurisson, *Chem. Rev.* **113**, 858 (2013).
- 4) J. Funkhouser, *Curr. Drug Discov.* **2**, 17 (2002).
- 5) Biogen Idec Inc., *Zevalin* (ibritumomab tiuxetan) (Biogen Idec Inc., San Deiego, CA, 2005).
- 6) J. J. Zaknun, L. Bodei, J. Mueller-Brand, M. E. Pavel, R. P. Baum, D. Horsch, T. M. O'Dorisio, J. R. Howe, M. Cremonesi, and D. J. Kwekkeboom, *Eur. J. Nucl. Med. Mol. Imaging* **40**, 800 (2013).
- 7) M.-M. Bé, V. Chisté, C. Dulieu, E. Browne, V. Chechev, N. Kuzmenko, R. Helmer, A. Nichols, E. Schönfeld, and R. Dersch, *Table of Radionuclides*, Monographie BIPM-5 (Vol. 2-A = 151 to 242) (Bureau International des Poids et Mesures, Sèvres, 2004).
- 8) E. Seregni, M. Maccauro, C. Chiesa, L. Mariani, C. Pascali, V. Mazzaferro, F. De Braud, R. Buzzoni, M. Milione, A. Lorenzoni, A. Bogni, A. Coliva, S. Lo Vullo, and E. Bombardieri, *Eur. J. Nucl. Med. Mol. Imaging* **41**, 223 (2014).
- 9) C. Cullinane, C. M. Jeffery, P. D. Roselt, E. M. van Dam, S. Jackson, K. Kuan, P. Jackson, D. Binns, J. van Zuylenkom, M. J. Harris, R. J. Hicks, and P. S. Donnelly, *J. Nucl. Med.* **61**, 1800 (2020).
- 10) P. S. Balasubramanian, *J. Radioanal. Nucl. Chem.* **185**, 305 (1994).
- 11) K. Hashimoto, H. Matsuoka, and S. Uchida, *J. Radioanal. Nucl. Chem.* **255**, 575 (2003).
- 12) T. Siiskonen, J. Huikari, T. Haavisto, J. Bergman, S.-J. Heselius, J.-O. Lill, T. Lönnroth, K. Peräjärvi, and V.-P. Varti, *Nucl. Instrum. Methods Phys. Res., Sect. B* **267**, 3500 (2009).
- 13) A. Hermanne, S. Takács, M. B. Goldberg, E. Lavie, Y. N. Shubin, and S. Kovalev, *Nucl. Instrum. Methods Phys. Res., Sect. B* **247**, 223 (2006).
- 14) S. Manenti, F. Groppi, A. Gandini, L. Gini, K. Abbas, U. Holzwarth, F.

- Simonelli, and M. Bonardi, *Appl. Radiat. Isot.* **69**, 37 (2011).
- 15) F. Tárkányi, F. Ditrói, S. Takács, A. Hermanne, H. Yamazaki, M. Baba, A. Mohammadi, and A. V. Ignatyuk, *Nucl. Instrum. Methods Phys. Res., Sect. B* **304**, 36 (2013).
  - 16) M. U. Khandaker, H. Haba, N. Otuka, and A. R. Usman, *Nucl. Instrum. Methods Phys. Res., Sect. B* **335**, 8 (2014).
  - 17) B. Király, F. Tárkányi, S. Takács, A. Hermanne, S. F. Kovalev, and A. V. Ignatyuk, *Nucl. Instrum. Methods Phys. Res., Sect. B* **266**, 3919 (2008).
  - 18) A. G. Kazakov, S. S. Belyshev, T. Yu. Ekatova, V. V. Khankin, A. A. Kuznetsov, and R. A. Aliev, *J. Radioanal. Nucl. Chem.* **317**, 1469 (2018).
  - 19) M. Fujita, T. Endo, H. Okamura, T. Shinozuka, H. Suzuki, E. Tanaka, A. Terakawa, A. Yamazaki, T. Miyake, S. Chiba, S. Kan, A. Matsumura, Y. Ohmiya, N. Takahashi, and S. Yokokawa, Proc. 17th International Conference on Cyclotrons and Their Applications, Tokyo, 2004, p. 143.
  - 20) J. Meija, T. B. Coplen, M. Berglund, W. A. Brand, P. De Bièvre, M. Gröning, N. E. Holden, J. Irrgeher, R. D. Loss, T. Walczyk, and T. Prohaska, *Pure Appl. Chem.* **88**, 293 (2016).
  - 21) M. J. Berger, J. H. Hubbell, S. M. Seltzer, J. Chang, J. S. Coursey, R. Sukumar, D. S. Zucker, and K. Olsen, XCOM Photon Cross Sections Database [<http://physics.nist.gov/PhysRefData/Xcom/html/xcom1.html>].
  - 22) A. Abbott, C. G. Sakellis, E. Andersen, Y. Kuzuhara, L. Gilbert, K. Boyle, M. H. Kulke, J. A. Chan, A. Jacene, and A. D. Van den Abbeele, *J. Nucl. Med. Technol.* **46**, 237 (2018).
  - 23) T. Sato, Y. Iwamoto, S. Hashimoto, T. Ogawa, T. Furuta, S. Abe, T. Kai, P. Tsai, N. Matsuda, H. Iwase, N. Shigyo, L. Sihver, and K. Niita, *J. Nucl. Sci. Technol.* **55**, 684 (2018).
  - 24) K. Hashimoto, private communication.